THE JOURNAL OF BIOLOGICAL CHEMISTRY VOL. 287, NO. 9, pp. 6084–6088, February 24, 2012

Z-Phe-Ala-diazomethylketone (PADK) Disrupts and Remodels Early Oligomer States of the Alzheimer Disease Aβ42 Protein*[S]

Received for publication, November 28, 2011, and in revised form, January 10, 2012
Published, JBC Papers in Press, January 17, 2012, DOI 10.1074/jbc.C111.328575

Xueyun Zheng[‡], Megan M. Gessel[‡], Meagan L. Wisniewski[§], Kishore Viswanathan[¶‖], Dennis L. Wright[¶], Ben A. Bahr[§], and Michael T. Bowers[‡1]

From the [‡]Department of Chemistry and Biochemistry, University of California, Santa Barbara, California 93106-9510, the [§]William C. Friday Laboratory, Biotechnology Research and Training Center, University of North Carolina, Pembroke, North Carolina 28372-1510, the [¶]Department of Pharmaceutical Sciences, University of Connecticut, Storrs, Connecticut 06269, and [‖]Synaptic Dynamics Incorporated, Farmington, Connecticut 06032

Background: The early oligomer states of Aβ are the primary therapeutic target for AD.
Results: PADK binds to Aβ directly and inhibits and reverses the formation of dodecamer of Aβ42.
Conclusion: PADK disrupts and remodels the early oligomerization of Aβ42.
Significance: The study of PADK and Aβ42 provides an example of small molecule therapeutic development for AD and other amyloid diseases.

The oligomerization of the amyloid-β protein (Aβ) is an important event in Alzheimer disease (AD) pathology. Developing small molecules that disrupt formation of early oligomeric states of Aβ and thereby reduce the effective amount of toxic oligomers is a promising therapeutic strategy for AD. Here, mass spectrometry and ion mobility spectrometry were used to investigate the effects of a small molecule, Z-Phe-Ala-diazomethylketone (PADK), on the Aβ42 form of the protein. The mass spectrum of a mixture of PADK and Aβ42 clearly shows that PADK binds directly to Aβ42 monomers and small oligomers. Ion mobility results indicate that PADK not only inhibits the formation of Aβ42 dodecamers, but also removes preformed Aβ42 dodecamers from the solution. Electron microscopy images show that PADK inhibits Aβ42 fibril formation in the solution. These results are consistent with a previous study that found that PADK has protective effects in an AD transgenic mouse model. The study of PADK and Aβ42 provides an example of small molecule therapeutic development for AD and other amyloid diseases.

Alzheimer disease (AD)[2] is the leading cause of late life dementia and is characterized as a progressive brain disorder that damages synapses and eventually destroys brain cells (1, 2). The aggregation of amyloid-β protein (Aβ) into soluble oligomeric species has been implicated as a key step in AD pathogenesis (3). Among the Aβ peptides that exist *in vivo*, the 42-amino acid Aβ42 has been found to be the primary component of amyloid deposits that are a hallmark of AD (4). Recently, increasing evidence shows that the early oligomeric states rather than the later stage fibrillization of Aβ42 are implicated in the onset of AD (5–8). Aβ42 monomers form small oligomers in solution, as well as paranuclei (pentamers and hexamers) that self-assemble to form decamers and dodecamers (9–14). An *in vivo* study identified a 56-kDa Aβ species (corresponding to a dodecamer) as the cause of memory disruption in affected mice (15). Because of their role in neuronal pathology, early oligomers of Aβ42 are a primary therapeutic target for AD.

A critical aspect of AD treatment and prevention is the clearance of Aβ proteins and protein aggregates from the brain (16). This clearance can be accomplished by directly disrupting the aggregation of Aβ proteins or by the degradation of Aβ proteins by proteases. Numerous natural proteins, peptides, and small molecules have been found to interfere with Aβ and disrupt the aggregation pathway (17). Small molecules are particularly attractive as a direct therapeutic strategy for the treatment of amyloidosis (18–20). They include known bioactive molecules (for example, curcumin (21) and (−)-epigallocatechin gallate (22)) and polyphenols (23, 24). On the other hand, Aβ-degrading enzymes have been investigated to understand the proteolysis in AD and targeted for therapeutic intervention (25). In this respect, lysosomal enzymes play an important role in protein degradation and clearance (26, 27). One of these enzymes, cathepsin B, has been shown to have anti-amyloidogenic and neuroprotective functions (28, 29). Recently, a small molecule, Z-Phe-Ala-diazomethylketone (PADK; the chemical structure is shown in Fig. 1*b*), has been investigated for its up-regulation of the lysosomal system (30). In AD transgenic mouse models (29), PADK was shown to selectively increase the cathepsin B level in the central nervous system. This resulted in reduced Aβ42 levels in the brain, which in turn offset the defects in synaptic composition and cognitive functions in the two transgenic models expressing different levels of Aβ pathology.

In the current study, we tested whether PADK directly interacts with Aβ itself. Also, we examined whether such interaction influences Aβ oligomerization and aggregation, in addition to the positive effect of PADK on the lysosomal system. Such a direct effect would provide evidence for the positive impact of PADK in AD pathology and provide an example of small molecule therapeutic development for AD and other amyloid diseases.

Recently, ion mobility spectrometry-mass spectrometry (IMS-MS) (31) has been successfully used to study the structure

* This work was supported, in whole or in part, by National Institutes of Health Grants IPOIAG 027818-010003 (to M. T. B.) and R25 GM077634 (to B. A. B.). This work was also supported by the Institute for the Study of Aging (to B. A. B.).
[S] This article contains supplemental text and Figs. S1–S4.
[1] To whom correspondence should be addressed. Tel.: 805-893-2893; Fax: 805-893-8703; E-mail: bowers@chem.ucsb.edu.

[2] The abbreviations used are: AD, Alzheimer disease; Aβ, amyloid-β protein; PADK, Z-Phe-Ala-diazomethylketone (Z, benzyloxycarbonyl); IMS, ion mobility spectrometry; ATD, arrival time distribution.

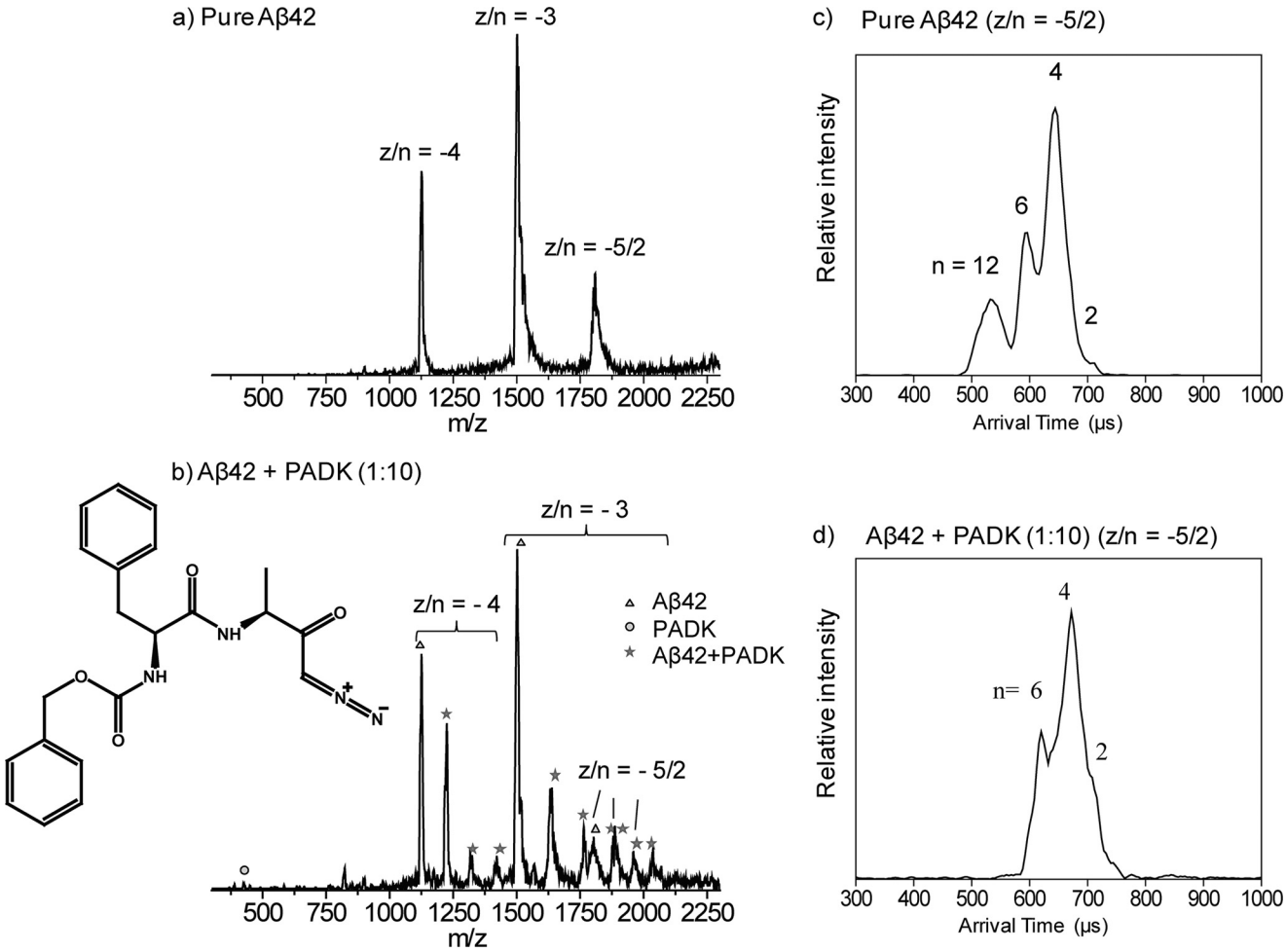

FIGURE 1. *a*, mass spectrum of pure Aβ42. *b*, mass spectrum of a 1:10 mixture of Aβ42 and PADK (PADK molecule structure included). Aβ42 peaks are represented by *triangles*, PADK peaks are represented by the *circle*, and the peaks due to the complex of Aβ42 and PADK are represented by *stars*. *z*/*n* is noted for each peak, where *z* is the charge and *n* is the oligomeric number. *c* and *d*, ATDs for $z/n = -5/2$ of Aβ42. *c*, pure Aβ42. *d*, 1:10 mixture of Aβ42 and PADK. Oligomeric order (*n*) is noted for each feature.

and aggregation of amyloid systems (32–36), including amyloid-β protein (12, 13, 35, 37, 38). In this work, we use IMS-MS to elucidate the interaction of PADK and Aβ42.

EXPERIMENTAL PROCEDURES

Sample Preparation—Aβ42 was synthesized using 9-fluorenylmethyloxycarbonyl-based methods (39), and PADK was obtained from Bachem Americas, Inc. (N-1040; Torrance, CA). Aβ42 and PADK were allowed to interact with each other by premixing in ammonium acetate buffer (7.5 mM, pH = 7.4) with a 1:10 ratio. To slow down the aggregation process for better signal, the samples were kept on ice until the IMS experiment was performed.

Ion Mobility Spectrometry-Mass Spectrometry—The samples were analyzed on a home-built ion mobility mass spectrometer (40). IMS (31) is capable of separating species that have the same mass-to-charge ratio but different shapes and oligomer sizes (12, 13). In the IMS measurements, the ions are pulsed into a drift cell filled with helium gas and passed through the cell under the influence of a weak electronic field. The species are separated in time according their sizes, and their arrival times at the detector are measured.

Electron Microscopy (EM)—All the Aβ42 samples were exactly the same ones as used in the IMS experiments and kept in a refrigerator for 2 weeks after IMS experiments. 10 μl of samples were drop-casted to the silicon chips and analyzed by scanning electron microscopy.

RESULTS

Mass spectra were recorded to determine whether PADK binds to Aβ42. The mass spectrum of a 1:10 mixture of Aβ42 and PADK is shown in Fig. 1*b* (see supplemental Figs. S2 and S3 for the results of the 1:1 ratio). In the mass spectrum, there are three peaks corresponding to Aβ42 $z/n = -4$, -3, and $-5/2$ (z = charge, n = oligomer size), which is similar to the pure Aβ42 mass spectrum (Fig. 1*a*). The peak at $m/z = 394$ represents pure PADK. Peaks trailing the $z/n = -4$ and -3 peaks of Aβ42 labeled with *stars* represent Aβ42-PADK complexes. For $z/n = -4$, peaks representing Aβ42 monomer with one, two, and three PADK molecules bound are observed, whereas for the $z/n = -3$, there are peaks corresponding to Aβ42 monomer with one, two, three, and four PADK molecules bound. For $z/n = -5/2$, there are two Aβ42-PADK complex peaks (m/z = 1884 and 1963), corresponding to Aβ42 dimer with one and two PADK molecules bound, respectively. Overall, the mass spectrum clearly shows that the PADK molecule binds directly to Aβ42. Moreover, the ratio of the -3 monomer peak to the $-5/2$

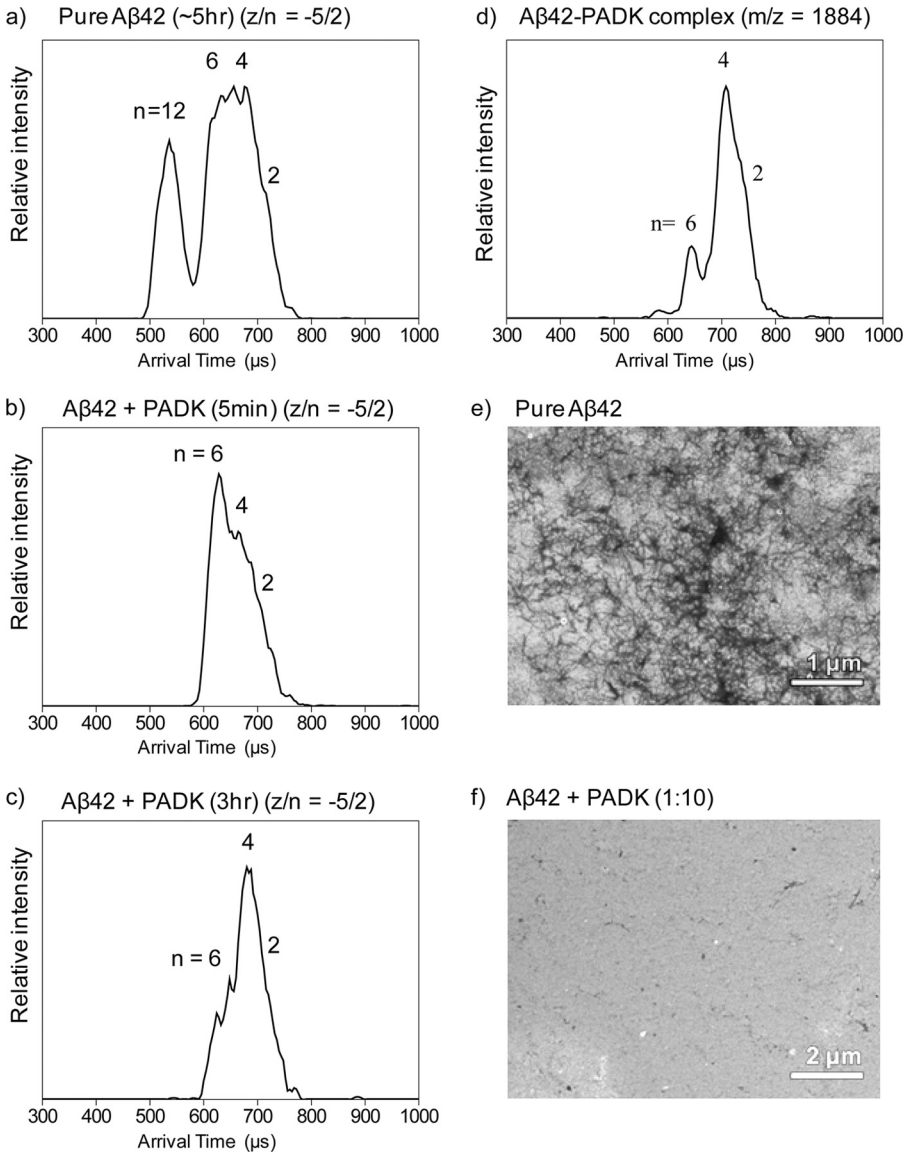

FIGURE 2. *a–c*, ATDs of $z/n = -5/2$ of Aβ42 in a time-course study of recovery of aggregated Aβ42 by PADK. *a*, Aβ42 without PADK on ice for ~5 h. *b*, 5 min after PADK was added to the same aggregated Aβ42 sample. *c*, 3 h after PADK was added to the aggregated Aβ42 sample. *d*, ATD of $z/n = -5/2$ of the Aβ42-PADK complex (2:1) peak at $m/z = 1884$. EM images of fibrils of Aβ42 samples that were kept in a refrigerator for 2 weeks are shown. *e*, Aβ42 sample without PADK. The dark regions are Aβ fibrils and plaques. *f*, 1:10 mixture of Aβ42 and PADK. Essentially no fibrils are observed.

peak in the Aβ42 sample with PADK, 6.4 (Fig. 1*b*), is higher than that in the Aβ42 sample without PADK, 3.3 (Fig. 1*a*), which shows quantitatively that the Aβ42 monomer concentration is increasing in the solution relative to the aggregate concentration as the PADK relative concentration increases.

The arrival time distributions (ATDs) for the $z/n = -5/2$ peaks are given in Fig. 1, *c* and *d*. The Aβ42 sample without PADK (Fig. 1*c*) shows four features with arrival times at ~720, 680, 600, and 540 μs. No other peaks at lower arrival times are observed. These peaks have previously been assigned as the −5 dimer, −10 tetramer, −15 hexamer, and −30 dodecamer (See Refs. 12 and 13 for a detailed discussion of −5/2 peak assignment). In Fig. 1*d*, the ATD of the −5/2 charge state of Aβ42 in the mixture of Aβ42 and PADK shows three features, which are assigned as dimer, tetramer, and hexamer based on their measured collision cross-section. Notice that the feature corresponding to the Aβ42 dodecamer is absent in the presence of PADK, which indicates that the formation of the dodecamer is inhibited by PADK. No other peaks appear at shorter arrival times, suggesting that Aβ42 forms only through hexamer in the presence of PADK. After 2 days, the Aβ42/PADK mixture still shows strong signal as compared with pure Aβ42 sample, and the ATDs show that there are no large aggregates forming in the solution with PADK. (See supplemental data and supplemental Fig. S1).

To investigate whether PADK also has an effect on removal of preformed dodecamer from solution, PADK was added to a preaggregated Aβ42 sample. The ATD of the −5/2 peak was monitored over time. After several hours of aggregation, the ATD of the −5/2 peak of Aβ42 (Fig. 2*a*) shows dodecamer, hexamer, tetramer, and dimer features. Concentrated PADK was added to this same sample with 1:10 ratio and monitored over time. After the addition of PADK, the dodecamer feature in the ATD disappears, whereas hexamer, tetramer, and dimer features are maintained (Fig. 2*b*). At later times, the most abun-

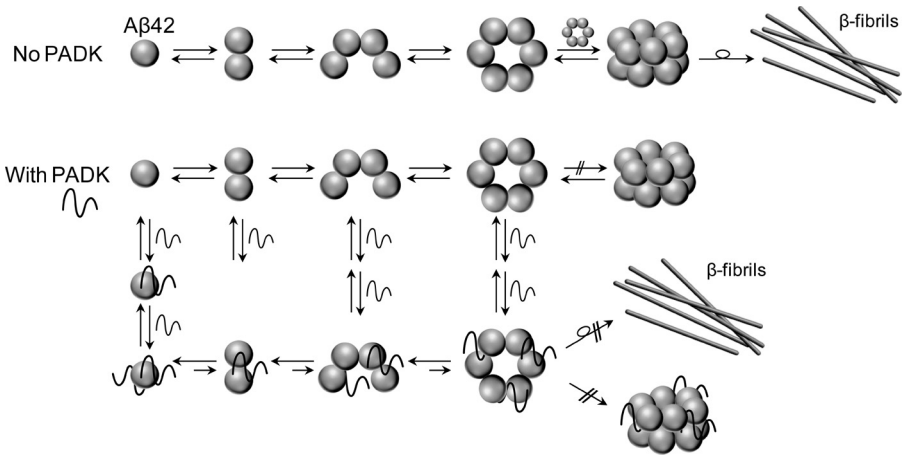

SCHEME 1. **Possible mechanism of inhibition of Aβ42 aggregation by PADK.** Neat samples of Aβ42 form dimer, tetramer, hexamer, and dodecamer and eventually form β-sheet fibrils in solution. PADK binds to not only Aβ42 monomer, but also dimer, tetramer, and hexamer, and thereby disrupts the formation of Aβ42 dodecamer, as well as the growth of fibrils. Over time, smaller oligomers (and monomers) become favored over larger oligomers (Figs. 1 and 2).

dant feature in the ATD shifts from hexamer to tetramer (Fig. 2*c*). The disappearance of dodecamer in this recovery experiment indicates that the PADK not only inhibits the formation of dodecamer but also removes preformed dodecamer in the solution. These results also suggest that PADK inhibits hexamer or paranucleus (11, 14) formation as well (Scheme 1).

The ATD of the −5/2 peak corresponding to an Aβ42-PADK complex (m/z = 1884) was also measured and is shown in Fig. 2*d*. (The signal of the m/z = 1963 peak corresponding to z/n = −5/2 with two PADKs attached was too low to record a reliable ATD; therefore the data are not shown here.) The ATD shows three features corresponding to dimer, tetramer, and hexamer, with one, two, and three PADKs bound, respectively. No dodecamer is present, which is similar to the result of z/n = −5/2 for Aβ42 (Fig. 1*d*). The result suggests that PADK not only to binds to Aβ42 monomer in the solution, but also binds to Aβ42 dimer, tetramer, and hexamer and thereby disrupts and reverses the formation of dodecamer and to a lesser degree the hexamer (Scheme 1).

EM was used to elucidate the effect of PADK on fibril formation. The EM images of both samples are given in Fig. 2, *e* and *f*. The Aβ42 sample shows substantial fibril formation and mass aggregates resembling plaque-like structures (they appear as darker areas in Fig. 2*e*). For the Aβ42 sample with PADK, no large aggregates are found, showing a much cleaner image in Fig. 2*f*. This indicates that there is less (if any) fibril formation in the solution with PADK, thus supporting our ion mobility data.

DISCUSSION

Mass spectra show that PADK binds to Aβ42 monomer and small oligomers directly. IMS-MS reveals that PADK not only inhibits the formation of the Aβ42 dodecamer but also removes preformed Aβ42 dodecamer in solution (Scheme 1). The ratio of the −3 monomer peak to the −5/2 peak increases in the Aβ42 sample with PADK, suggesting that the dodecamer is most likely converted into smaller species and eventually monomer. EM images indicate that PADK can also prevent the formation of Aβ42 fibrils. Our study is consistent with the study showing that PADK can help reduce the Aβ42 levels in the brain of AD transgenic mice and in turn improve their synaptic composition and cognitive function (29). In that AD transgenic mice study, PADK was observed to be a positive modulator that up-regulated the level of proteases, which in turn enhanced the clearance of Aβ42 species. On the other hand, our current study probed the direct relationship between PADK and Aβ42 and found that there is also a direct interaction involved in the positive effect of PADK on AD pathology. Perhaps the ability of PADK to disaggregate extracellular Aβ peptide leads to efficient uptake of monomers and small oligomers into neurons and microglia, thereby allowing trafficking to lysosomes for degradative detoxification by cysteine proteases (29, 30, 41). Theoretical studies on the interaction of PADK and Aβ42 are underway that will provide more structural information to better understand structure-neurotoxicity correlations of this system. Due to the aromatic nature of PADK, we suspect that perhaps PADK prefers to interact with the N-terminal region of Aβ that has a high content of aromatic residues (fragment 13–20 contains 2 His and 2 Phe residues). Such a binding mode has been suggested in a previous study (42). On the other hand, the hydrophobic nature of PADK might result in binding to the hydrophobic C-terminal region of Aβ. Finally, to gain a better understanding of the structure specificity of PADK on Aβ42 toxicity, a family of molecules with structures similar to PADK is under study. Preliminary results indicate a wide variety of responses of Aβ42 to these molecules and will be reported elsewhere when the study is finished. One EM image is included in supplemental Fig. S4*c* to indicate that the specific PADK structure is important, not just generic ring systems.

Acknowledgments—Deyu Liu in the Stucky laboratory in the Department of Chemistry and Biochemistry, University of California Santa Barbara, is acknowledged for help with taking EM images of the Aβ42 samples. Margaret Condron at University of California Los Angeles is acknowledged for the preparation of Aβ42 samples.

REFERENCES

1. Mattson, M. P. (2004) Pathways toward and away from Alzheimer disease. *Nature* **430,** 631–639
2. Stokin, G. B., Lillo, C., Falzone, T. L., Brusch, R. G., Rockenstein, E., Mount, S. L., Raman, R., Davies, P., Masliah, E., Williams, D. S., and Gold-

stein, L. S. (2005) Axonopathy and transport deficits early in the pathogenesis of Alzheimer disease. *Science* **307,** 1282–1288
3. Roychaudhuri, R., Yang, M., Hoshi, M. M., and Teplow, D. B. (2009) Amyloid-β protein assembly and Alzheimer disease. *J. Biol. Chem.* **284,** 4749–4753
4. Billings, L. M., Oddo, S., Green, K. N., McGaugh, J. L., and LaFerla, F. M. (2005) Intraneuronal Aβ causes the onset of early Alzheimer disease-related cognitive deficits in transgenic mice. *Neuron* **45,** 675–688
5. Klein, W. L., Krafft, G. A., and Finch, C. E. (2001) Targeting small Aβ oligomers: the solution to an Alzheimer disease conundrum? *Trends Neurosci.* **24,** 219–224
6. Walsh, D. M., Klyubin, I., Fadeeva, J. V., Cullen, W. K., Anwyl, R., Wolfe, M. S., Rowan, M. J., and Selkoe, D. J. (2002) Naturally secreted oligomers of amyloid-β protein potently inhibit hippocampal long-term potentiation *in vivo*. *Nature* **416,** 535–539
7. Kirkitadze, M. D., Bitan, G., and Teplow, D. B. (2002) Paradigm shifts in Alzheimer disease and other neurodegenerative disorders: the emerging role of oligomeric assemblies. *J. Neurosci. Res.* **69,** 567–577
8. Ono, K., Condron, M. M., and Teplow, D. B. (2009) Structure-neurotoxicity relationships of amyloid-β protein oligomers. *Proc. Natl. Acad. Sci. U.S.A.* **106,** 14745–14750
9. Bitan, G., Lomakin, A., and Teplow, D. B. (2001) Amyloid-β protein oligomerization: prenucleation interactions revealed by photo-induced cross-linking of unmodified proteins. *J. Biol. Chem.* **276,** 35176–35184
10. Teplow, D. B., Lazo, N. D., Bitan, G., Bernstein, S., Wyttenbach, T., Bowers, M. T., Baumketner, A., Shea, J. E., Urbanc, B., Cruz, L., Borreguero, J., and Stanley, H. E. (2006) Elucidating amyloid-β protein folding and assembly: a multidisciplinary approach. *Acc. Chem. Res.* **39,** 635–645
11. Bitan, G., Kirkitadze, M. D., Lomakin, A., Vollers, S. S., Benedek, G. B., and Teplow, D. B. (2003) Amyloid-β protein (Aβ) assembly: Aβ40 and Aβ42 oligomerize through distinct pathways. *Proc. Natl. Acad. Sci. U.S.A.* **100,** 330–335
12. Bernstein, S. L., Wyttenbach, T., Baumketner, A., Shea, J. E., Bitan, G., Teplow, D. B., and Bowers, M. T. (2005) Amyloid-β protein: monomer structure and early aggregation states of Aβ42 and its Pro-19 alloform. *J. Am. Chem. Soc.* **127,** 2075–2084
13. Bernstein, S. L., Dupuis, N. F., Lazo, N. D., Wyttenbach, T., Condron, M. M., Bitan, G., Teplow, D. B., Shea, J. E., Ruotolo, B. T., Robinson, C. V., and Bowers, M. T. (2009) Amyloid-β protein oligomerization and the importance of tetramers and dodecamers in the etiology of Alzheimer disease. *Nat. Chem.* **1,** 326–331
14. Bitan, G., Vollers, S. S., and Teplow, D. B. (2003) Elucidation of primary structure elements controlling early amyloid-β protein oligomerization. *J. Biol. Chem.* **278,** 34882–34889
15. Lesné, S., Koh, M. T., Kotilinek, L., Kayed, R., Glabe, C. G., Yang, A., Gallagher, M., and Ashe, K. H. (2006) A specific amyloid-β protein assembly in the brain impairs memory. *Nature* **440,** 352–357
16. Bates, K. A., Verdile, G., Li, Q. X., Ames, D., Hudson, P., Masters, C. L., and Martins, R. N. (2009) Clearance mechanisms of Alzheimer amyloid-β peptide: implications for therapeutic design and diagnostic tests. *Mol Psychiatry* **14,** 469–486
17. Stains, C. I., Mondal, K., and Ghosh, I. (2007) Molecules that target β-amyloid. *ChemMedChem* **2,** 1675–1692
18. Necula, M., Kayed, R., Milton, S., and Glabe, C. G. (2007) Small molecule inhibitors of aggregation indicate that amyloid-β oligomerization and fibrillization pathways are independent and distinct. *J. Biol. Chem.* **282,** 10311–10324
19. Hawkes, C. A., Ng, V., and McLaurin, J. (2009) Small molecule inhibitors of Aβ-aggregation and neurotoxicity. *Drug Develop. Res.* **70,** 111–124
20. Re, F., Airoldi, C., Zona, C., Masserini, M., La Ferla, B., Quattrocchi, N., and Nicotra, F. (2010) β-amyloid aggregation inhibitors: small molecules as candidate drugs for therapy of Alzheimer disease. *Curr. Med. Chem.* **17,** 2990–3006
21. Yang, F., Lim, G. P., Begum, A. N., Ubeda, O. J., Simmons, M. R., Ambegaokar, S. S., Chen, P. P., Kayed, R., Glabe, C. G., Frautschy, S. A., and Cole, G. M. (2005) Curcumin inhibits formation of amyloid-β oligomers and fibrils, binds plaques, and reduces amyloid *in vivo*. *J. Biol. Chem.* **280,** 5892–5901
22. Ehrnhoefer, D. E., Bieschke, J., Boeddrich, A., Herbst, M., Masino, L., Lurz, R., Engemann, S., Pastore, A., and Wanker, E. E. (2008) EGCG redirects amyloidogenic polypeptides into unstructured, off-pathway oligomers. *Nat. Struct. Mol. Biol.* **15,** 558–566
23. De Felice, F. G., Houzel, J. C., Garcia-Abreu, J., Louzada, P. R., Jr., Afonso, R. C., Meirelles, M. N., Lent, R., Neto, V. M., and Ferreira, S. T. (2001) Inhibition of Alzheimer disease β-amyloid aggregation, neurotoxicity, and *in vivo* deposition by nitrophenols: implications for Alzheimer therapy. *FASEB J.* **15,** 1297–1299
24. Porat, Y., Abramowitz, A., and Gazit, E. (2006) Inhibition of amyloid fibril formation by polyphenols: structural similarity and aromatic interactions as a common inhibition mechanism. *Chem. Biol. Drug Des.* **67,** 27–37
25. Higuchi, M., Iwata, N., and Saido, T. C. (2005) Understanding molecular mechanisms of proteolysis in Alzheimer disease: progress toward therapeutic interventions. *Biochim. Biophys. Acta* **1751,** 60–67
26. Nixon, R. A., Mathews, P. M., and Cataldo, A. M. (2001) The neuronal endosomal-lysosomal system in Alzheimer disease. *J. Alzheimers Dis.* **3,** 97–107
27. Bahr, B. A. (2009) Lysosomal modulatory drugs for a broad strategy against protein accumulation disorders. *Curr. Alzheimer Res.* **6,** 438–445
28. Mueller-Steiner, S., Zhou, Y., Arai, H., Roberson, E. D., Sun, B., Chen, J., Wang, X., Yu, G., Esposito, L., Mucke, L., and Gan, L. (2006) Antiamyloidogenic and neuroprotective functions of cathepsin B: implications for Alzheimer disease. *Neuron* **51,** 703–714
29. Butler, D., Hwang, J., Estick, C., Nishiyama, A., Kumar, S. S., Baveghems, C., Young-Oxendine, H. B., Wisniewski, M. L., Charalambides, A., and Bahr, B. A. (2011) Protective effects of positive lysosomal modulation in Alzheimer disease transgenic mouse models. *PLoS ONE* **6,** e20501
30. Bahr, B. A., Wisniewski, M. L., and Butler, D. (2012) *Rejuvenation Res.*, in press
31. Wyttenbach, T., and Bowers, M. T. (2003) Gas-phase conformations: The ion mobility/ion chromatography method. *Top. Curr. Chem.* **225,** 207–232
32. Dupuis, N. F., Wu, C., Shea, J. E., and Bowers, M. T. (2009) Human islet amyloid polypeptide monomers form ordered β-hairpins: a possible direct amyloidogenic precursor. *J. Am. Chem. Soc.* **131,** 18283–18292
33. Grabenauer, M., Wyttenbach, T., Sanghera, N., Slade, S. E., Pinheiro, T. J., Scrivens, J. H., and Bowers, M. T. (2010) Conformational stability of Syrian hamster prion protein PrP(90–231). *J. Am. Chem. Soc.* **132,** 8816–8818
34. Grabenauer, M., Wu, C., Soto, P., Shea, J. E., and Bowers, M. T. (2010) Oligomers of the prion protein fragment 106–126 are likely assembled from β-hairpins in solution, and methionine oxidation inhibits assembly without altering the peptide's monomeric conformation. *J. Am. Chem. Soc.* **132,** 532–539
35. Baumketner, A., Bernstein, S. L., Wyttenbach, T., Bitan, G., Teplow, D. B., Bowers, M. T., and Shea, J. E. (2006) Amyloid-β protein monomer structure: a computational and experimental study. *Protein Sci.* **15,** 420–428
36. Dupuis, N. F., Wu, C., Shea, J. E., and Bowers, M. T. (2011) The amyloid formation mechanism in human IAPP: dimers have β-strand monomer-monomer interfaces. *J. Am. Chem. Soc.* **133,** 7240–7243
37. Murray, M. M., Bernstein, S. L., Nyugen, V., Condron, M. M., Teplow, D. B., and Bowers, M. T. (2009) Amyloid-β protein: Aβ40 inhibits Aβ42 oligomerization. *J. Am. Chem. Soc.* **131,** 6316–6317
38. Bleiholder, C., Dupuis, N. F., Wyttenbach, T., and Bowers, M. T. (2011) Ion mobility mass spectrometry reveals a conformational conversion from random assembly to β-sheet in amyloid fibril formation. *Nat. Chem.* **3,** 172–177
39. Lomakin, A., Chung, D. S., Benedek, G. B., Kirschner, D. A., and Teplow, D. B. (1996) On the nucleation and growth of amyloid-β protein fibrils: detection of nuclei and quantitation of rate constants. *Proc. Natl. Acad. Sci. U.S.A.* **93,** 1125–1129
40. Wyttenbach, T., Kemper, P. R., and Bowers, M. T. (2001) Design of a new electrospray ion mobility mass spectrometer. *Int. J. Mass Spectrom.* **212,** 13–23
41. Yang, C. N., Shiao, Y. J., Shie, F. S., Guo, B. S., Chen, P. H., Cho, C. Y., Chen, Y. J., Huang, F. L., and Tsay, H. J. (2011) Mechanism mediating oligomeric Aβ clearance by naive primary microglia. *Neurobiol. Dis.* **42,** 221–230
42. Convertino, M., Vitalis, A., and Caflisch, A. (2011) Disordered binding of small molecules to Aβ12–28. *J. Biol. Chem.* **286,** 41578–41588